Pergamon

Tetrahedron, Vol. 53, No. 29, pp. 10133-10154, 1997

0040-4020/97 $17.00 + 0.00

PII: S0040-4020(97)00354-2

SOLUTION AND SOLID STATE STUDIES OF SOME NEW SILICON AND GERMANIUM COMPOUNDS STABILIZED BY TRIDENTATE LIGANDS

Vladimir A. Benin[#], James C. Martin and M. Robert Willcott[##]*

Department of Chemistry, Vanderbilt University, Nashville, TN 37235

Abstract: The preparation and studies of novel heterocyclic compounds, containing silicon or germanium, is described. All of them incorporate the 2,6-bis(dialkylaminomethyl)-4-(1,1-dimethylethyl)phenyl tridentate ligand (Structures **1** - **2**, Scheme 1) as a main substructure. The report furnishes sets of experimental data that further clarify the actual solution and solid state structures of these new molecules with potentially hypervalent silicon or germanium centers.

INTRODUCTION

The preparation of hypervalent compounds of the Group IVA elements with trigonal bipyramidal geometry has been of considerable interest to us and a number of other groups.[1 - 5] The interest stems from the fact that the expected structure of these compounds resembles in geometry the S_N2 transition state. A large body of theoretical work, done in recent years to clarify and generalize the theory of hypervalency, has concentrated on model compounds containing pentavalent central atoms of elements from Group IVA.

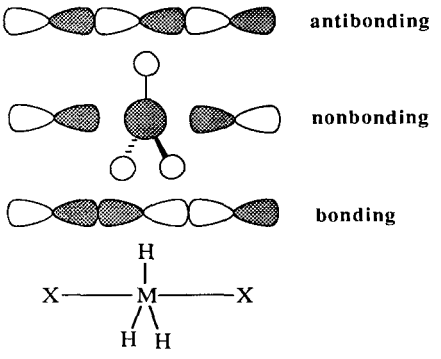

Figure 1. A modified 3c-4e bonding scheme.

The theoretical investigations have led to the introduction of new models of hypervalency which incorporate the idea of the three-center four-electron bond.[6 - 9] The new element is the participation of equatorial ligands in the hypervalent bonding scheme realized by the overlap of the classical nonboding orbital within the Musher-Rundle approach with an antibonding orbital distributed over the central atom and the equatorial substituents. Shaik and coworkers reached to this conclusion after extensive valence-bond computations of CH_5^- and SiH_5^- and the proposed by them modified 3c-4e bonding diagram is shown in Figure 1.[9, 10] Reed and von Schleyer propose the same idea (which they have termed negative hyperconjugation) after theoretical studies of hypervalent molecules with π-electrons.[11]

We have reported the synthesis of new potentially hypervalent silicon species by means of the tridentate ligand **1** (Scheme 1).[1] Ligand **1** is very similar to the "pincer" ligand of G. van Koten[12] but it is better suited for extensive, variable temperature NMR studies. The replacement of the proton at the 4-position of the benzene ring with a tertiary butyl group simplifies considerably the NMR spectrum and allows for easier, more precise monitoring of the aromatic resonances in the final compounds which has proved important for the low temperature NMR measurements.

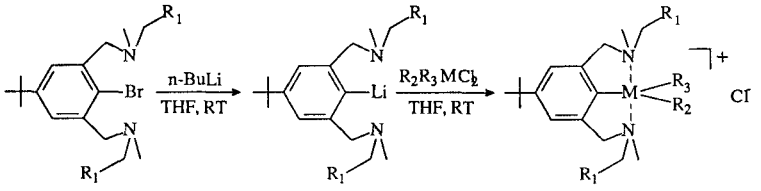

1: $R_1 = H$

2: $R_1 = CD_3$

3: M = Si, $R_2 = R_3 = CH_3$, $R_1 = H$

4: M = Si, $R_2 = CH_3$, R_3 = vinyl, $R_1 = H$

5: M = Ge, $R_2 = R_3 = CH_3$, $R_1 = H$

6: M = Ge, $R_2 = R_3 =$ 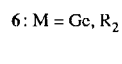 , $R_1 = H$

7: M = Ge, $R_2 = R_3 = CH_3$, $R_1 = CD_3$

Scheme 1. A general synthetic sequence for the preparation of compounds **3** - **7**.

The NMR properties of compound **3**, discussed previously, revealed the presence of the tetravalent asymmetrical forms **3a** and **3a'** in solution in a process of rapid dynamic equilibrium instead of the expected hypervalent structure **3b** (Figure 2). Parallel studies were conducted on similar compounds by Corriu and coworkers.[13] The authors, on the basis of room temperature NMR spectra in chloroform-*d* and conductivity measurements, asserted originally that the compounds prepared by them contained a silicon atom in a pentavalent state ("siliconium" ions)[13a], but more recent work by the same group has confirmed our conclusions about the structures of the species in solution.[13b]

There are in fact two general, fundamentally different hypotheses by means of which compounds **3** and **4**, as well as the molecules prepared by Corriu and coworkers, can be described. According to hypothesis 1, the molecules exist in a state with tetravalent silicon atom. Two identical forms in a 1:1 ratio are involved in a process of rapid equilibrium (Figure 2a). The symmetrical pentavalent structure is a transition state along the reaction coordinate of an S_N2-like identity exchange. According to hypothesis 2, the identity exchange proceeds through an intermediate which is the symmetrical form (Figure 2b). If the intermediate is sufficiently stabilized, it may become lower in energy compared to the open forms in which case it can be termed as a "frozen transition state". The explanation, originally suggested by Corriu and coworkers, obviously supports the "frozen transition state" hypothesis. Our conclusions as well as their later observations are consistent with hypothesis 1.

Compounds **5**, **6** and **7** contain germanium atom as a potential hypervalent center. The atomic properties of silicon and germanium, covalent radii, electronegativities and ionization potentials, are strikingly similar.[14] Thus, it was of particular interest to prepare and study germanium compounds derived on the basis of the same or similar tridentate ligand.

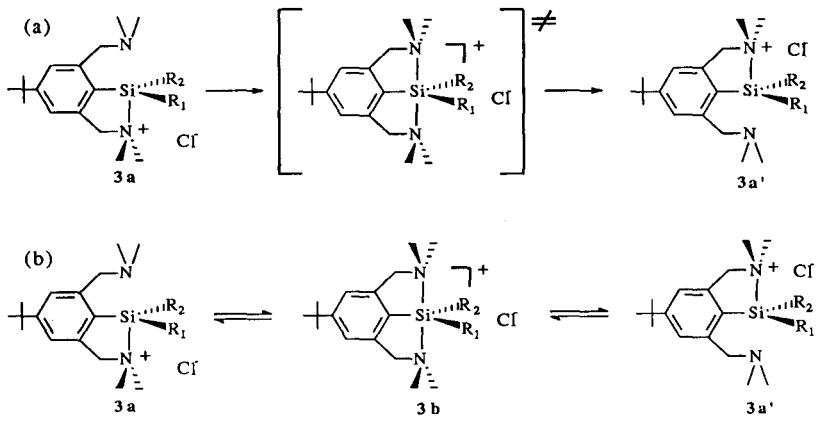

Figure 2. Two hypotheses for the state of the silicon-containing species **3** and **4** in solution.

EXPERIMENTAL

General Remarks. The variable temperature ^{1}H and ^{13}C NMR measurements were performed on Bruker AM400 spectrometer. The ^{29}Si NMR spectra were measured on Bruker AC200 and Bruker AM400 spectrometers. ^{15}N NMR spectra were obtained on Bruker AM400 spectrometer. Chemical shifts are reported in ppm (on the δ-scale) relative to TMS (0 ppm) for the ^{1}H, ^{13}C and ^{29}Si-spectra. The ^{29}Si spectra were run without the actual presence of TMS in the studied solutions. Instead, preliminary measurements were done with TMS in a variety of solvents in order to obtain the corresponding spectrum reference (SR) values which were subsequently used for the standardization of spectra of the investigated compounds. All silicon spectra were acquired by using an inverse-gated decoupling technique (INVGATE).[15] The ^{15}N spectra were referenced to liquid ammonia (0 ppm at 25°C). The actual standardization was indirect, based on the SR values for NH_4NO_3 in D_2O (δ_{NO_3} = 376.25 ppm) and conversion tables from the literature.[16] X-ray structural analysis was performed on AFC6S diffractometer with graphite monochromatic Mo Kα radiation. Mass spectra were obtained on a HEWLETT-PACKARD 5890 SERIES II GC-MS instrument. High-resolution mass spectrometry studies were done on KRATOS 4-SECTOR DOUBLE-FOCUSING instrument. The spectra were run in the positive Fast-Atom Bombardment (FAB) mode with a Cs-atoms source. The samples were studied in a glycerol/DMSO/3NBA matrix. Melting points were measured on BÜCHI 510 melting point apparatus. The tetrahydrofuran used in the synthesis of the final compounds was doubly dried over Na/benzophenone followed by $LiAlH_4$. Inert atmosphere was achieved by use of dry nitrogen gas. Some of the silicon- and germanium-containing precursors were purchased from ALDRICH Chemical Co.

2,6 - Bis(Dimethylaminomethyl)-4-(1,1-dimethylethyl)phenyl lithium (1). 2,6 - Bis(Dimethylaminomethyl)-4-(1,1-dimethylethyl)bromobenzene[1] (0.39 g, 0.0012 mol) was dissolved in dry THF (10 mL) in a 25 mL 3-neck round-bottomed flask equipped with magnetic stirrer, addition funnel and under inert atmosphere. n-BuLi (0.74 ml, 0.0012 mol, 1.6 M solution in hexane) was added dropwise at RT. The resulting solution was stirred for 1 h. An aliquot quenched with D_2O showed more than 95% incorporation of deuterium according to the ^{1}H NMR spectrum. ^{1}H NMR (chloroform-*d*) δ 7.20 (s, 2H), 3.41 (s, 4H), 2.23 (s, 12H), 1.32 (s, 9H).

C, N, N'-[2,6-Bis(Dimethylaminomethyl)-4-(1,1-dimethylethyl)phenyl]dimethyl siliconium chloride (3). Dichlorodimethylsilane (0.15 g, 0.0012 mol, 0.14 mL) was dissolved in dry THF (5 mL) in a 25 mL 3-neck round-

bottomed flask equipped with magnetic stirrer, addition funnel and under inert atmosphere. The solution of **1** from the previous experiment was added dropwise to the resulting mixture at room temperature. A white solid precipitated immediately. The mixture was stirred for 4 h, filtered and the white solid was crystallized from DMSO to yield 0.28 g (0.0008 mol, 69%) of colorless crystals. m.p. 240 - 242°C. ^{1}H NMR (DMSO-d_6) δ 7.30 (s, 2H), 3.98 (s, 4H), 2.47 (s, 12H), 1.30 (s, 9H), 0.57 (s, 6H); ^{13}C NMR (DMSO-d_6) δ 155.8, 144.0, 125.3, 121.1, 63.7, 46.1, 34.9, 31.0, -4.7; ^{29}Si NMR (DMSO-d_6) δ -2.61; Elem. Analysis: Calcd. ($C_{18}H_{33}ClN_2Si.H_2O$) C 60.22, H 9.83, N 7.80; Found ($C_{18}H_{33}ClN_2Si.H_2O$) C 60.02, H 9.70, N 7.53; MS $C_{18}H_{33}ClN_2Si$ Calcd.: M^+ = 340; Found: *m/z* 305 (M^+ - Cl).

C, N, N'-[2,6-Bis(Dimethylaminomethyl)-4-(1,1-dimethylethyl)phenyl]methylvinyl siliconium chloride (4). A solution of **1** in THF prepared from **6** (0.97 g, 0.0030 mol) and n-BuLi (1.85 mL, 0.00296 mol) was added dropwise to a solution of dichloromethylvinylsilane (0.42 g, 0.0030 mol, 0.39 mL) in THF at room temperature under nitrogen atmosphere. A white solid precipitated and the resulting mixture was stirred for additional 4 h. The solid material was separated by vacuum filtration and dried to yield 0.40 g (0.00112 mol, 38%). m.p. 196 - 198°C. ^{1}H NMR (D_2O) δ 7.49 (s, 2H), 6.39 (m, 1H), 6.15 (dd, 1H, J_1 = 3.43 Hz, J_2 = 14.80 Hz), 5.90 (dd, 1H, J_1 = 3.43 Hz, J_2 = 20.30 Hz), 4.28 (s, 4H), 2.64 (s, 12H), 1.21 (s, 9H), 0.45 (s, 3H); ^{13}C NMR (methanol-d_4) δ 154.7, 136.8, 135.1, 133.0, 130.2, 65.1, 43.9, 35.4, 31.3, -3.6; MS $C_{19}H_{33}ClN_2Si$ Calcd.: M^+ = 352; Found: *m/z* 317 (M^+ - Cl).

1-Bromo-4-(1,1-dimethylethyl)-2,6-benzenedicarboxylic acid (9). 2,6-dimethyl-4-(1,1-dimethylethyl)bromobenzene (10 g, 0.0415 mol) was placed in a 500 mL 3-neck flask and 300 mL of 1:1 (v/v) mixture of water and *t*-butanol was added. The mixture was stirred and heated until all the starting material dissolves. $KMnO_4$ (14 g, 0.0886 mol) was added and the resulting mixture heated at reflux for 1 h followed by addition of the rest of $KMnO_4$ (13 g, 0.0820 mol; total of 27 g or 0.1706 mol). The reflux was continued for 14 h. The mixture was cooled to RT and MnO_2 was separated by vacuum filtration. This solution was concentrated to half of its original volume and acidified with conc. HCl. The precipitate was collected and dried to yield 10.20 g (0.0339 mol, 82%) of white solid, m.p. 237 - 239°C. ^{1}H NMR (acetonitrile-d_3) δ 9.80 (broad s, 2H), 7.76 (s, 2H), 1.30 (s, 9H); ^{13}C NMR (acetone-d_6) δ 168.1, 151.8, 137.0, 129.5, 114.4, 36.3, 31.1; MS *m/e* (relative intensity) 302 (14.0, $(M + 2)^+$), 300 (16.0, M^+), 287 (98.0, $(M + 2)^+ - CH_3$), 285 (100, $M^+ - CH_3$), 257 (20.0, $M^+ - CH_3 - H_2O$).

1-Bromo-4-(1,1-dimethylethyl)-2,6-benzenedicarboxylic acid dichloride (10). 1-bromo-4-(1,1-dimethylethyl)-2,6-benzenedicarboxylic acid (**9**) (5.00 g, 0.0166 mol) and PCl_5 (6.92 g, 0.0332 mol) were mixed in the solid state in a 50 mL round-bottomed flask equipped with a condenser and a drying tube. The flask was immersed in oil bath heated to 150°C. A vigorous reaction takes place and the solid mixture turned into a homogenous liquid which was heated for additional 0.5 h. The side product, $POCl_3$, was removed under reduced pressure at 150°C. The remaining liquid solidified upon rapid cooling to -20°C. Petroleum ether was added to dissolve the solid material and the resulting solution left for 12 h at -20°C. Large needle-type crystals formed. They were collected by vacuum filtration and dried to yield 4.05 g (0.0120 mol, 72%) of pure dichloride. m.p. 45 - 46°C. ^{1}H NMR (benzene-d_6) δ 7.53 (s, 2H), 0.83 (s, 9H); ^{13}C NMR (benzene-d_6) δ 166.0, 151.8, 138.7, 131.1, 114.2, 34.6, 30.3; MS *m/e* (relative intensity) 340 (1.6, $(M+4)^+$), 338 (2.6, $(M+2)^+$), 336 (2.1, M^+), 327 (0.5, $(M+6)^+ - CH_3$), 325 (5.1, $(M+4)^+ - CH_3$), 323 (10.8, $(M+2)^+ - CH_3$), 321 (7.2, $M^+ - CH_3$), 305 (24.2, $(M+4)^+$ - Cl), 303 (100, $(M+2)^+$ - Cl), 301 (78.9, M^+ - Cl).

1-Bromo-4-(1,1-dimethylethyl)-2,6-benzenedicarboxylic acid, bis (N,N-dimethyl amide), ^{15}N labeled (11). 1-Bromo-4-(1,1-dimethylethyl)-2,6-benzenedicarboxylic acid dichloride (**10**) 2.10 g (0.0061 mol) was dissolved in 50 mL of dichloromethane and the solution transferred into a 100 mL 3-neck round-bottomed flask equipped with a cold finger condenser (dry ice/iso-propanol mixture) and addition funnel. Dimethylamine hydrochloride (1.00 g, 0.0123 mol, 99% ^{15}N) was

added to the solution and the system was immersed in an ice/water bath. Triethylamine (2.50 g, 0.0246 mol, 3.45 mL) 10 mL of CH_2Cl_2 was added dropwise to the mixture. A white solid precipitated after about 5 min. The stirring was continued for 3 h while warming to room temperature. The mixture was poured into an equal volume of water to dissolve the triethylamine hydrochloride. The organic layer was separated and the aqueous layer extracted with 50 mL of ether. The organic layers were combined and dried over Mg_2SO_4. Removal of solvent yielded product as a white solid (2.05 g, 0.0058 mol, 94%) used for the next step without further purification. m.p. 196 - 198°C. ^{1}H NMR (chloroform-*d*) δ 7.28 (s, 2H), 3.14 (d, 6H, J = 1.01 Hz), 2.86 (d, 6H, J = 0.94 Hz), 1.30 (s, 9H); ^{13}C NMR (chloroform-*d*) δ 169.0 (d, J = 17.22 Hz), 152.1, 139.1 (d, J = 7.84 Hz), 125.0, 112.5, 38.2 (d, J = 11.50 Hz), 34.8, 34.5 (d, J = 10.92 Hz); MS *m/e* (relative intensity) 358 (7.7, $(M+2)^+$), 356 (8.2, M^+), 313 (98.5, $(M+2)^+$ - $^{15}N(CH_3)_2$), 311 (100, M^+ - $^{15}N(CH_3)_2$), 277 (34.5, M^+ - Br), 73 (38.7, $CO^{15}N(CH_3)_2^+$).

2,6-Bis(Dimethylaminomethyl)-4-(1,1-dimethylethyl)bromobenzene, ^{15}N labeled (12). Compound **11** (1.05 g, 0.0030 mol) was dissolved in anhydrous THF and transferred into a 100 mL 3-neck flask equipped with addition funnel and under inert atmosphere. BH_3.THF (9.87 mL, 0.0099 mol, 1 M solution in THF) was added dropwise at 0 - 5°C. The resulting solution was stirred for 40 h at room temperature. 6N HCl (5 mL) was then added dropwise. The mixture was heated to reflux and THF was distilled. A small amount of water was added followed by extraction with ether (2 x 20 mL). The layers were separated, concentrated KOH was added to the aqueous layer until alkaline reaction (pH = 12 - 13) and the mixture extracted with ether (2 x 50 mL). The combined organic layers were dried over $MgSO_4$ and the solvent was removed under reduced pressure. The residue was crystallized from DMSO and dried to yield 0.75 g (0.0023 mol, 77%) of white crystalline solid. ^{15}N NMR (chloroform-*d*) δ 25.95

C, N, N'-[2,6-Bis(Dimethylaminomethyl)-4-(1,1-dimethylethyl)phenyl]dimethyl germanium chloride (5). A solution of **1** in THF prepared from 2,6-bis(dimethylaminomethyl)-4-(1,1-dimethylethyl)bromobenzene (0.52 g, 0.0016 mol) and n-BuLi (1.00 mL, 0.0016 mol) was added dropwise to a solution of dimethylgermanium dichloride (0.28 g, 0.0016 mol, 0.18 mL) in THF at RT under nitrogen atmosphere. The mixture was stirred for 4h and the white precipitation was separated by vacuum filtration. The solid material was further crystallized from DMSO to yield 0.43 g (0.0011 mol, 71%) of white solid. m.p. 286 - 288°C. ^{1}H NMR (methanol-*d4*) δ 7.34 (s, 2H), 3.88 (s, 4H), 2.49 (s, 12H), 1.33 (s, 9H), 0.95 (s, 6H); ^{13}C NMR (D_2O) δ 156.4, 142.3, 128.0, 122.3, 63.2, 45.3, 34.5, 30.4, -2.5; Elem. Analysis: 1.Recrystallized from DMSO: Calcd. ($C_{18}H_{33}ClGeN_2.H_2O$) C 53.57, H 8.74, N 6.94; Found: ($C_{18}H_{33}ClGeN_2.H_2O$) C 53.33, H 8.54, N 6.87; 2.Crystallized from CH_2Cl_2: Calcd. ($C_{18}H_{33}ClGeN_2.0.60\ CH_2Cl_2$) C 51.18, H 7.90, 6.42; Found: ($C_{18}H_{33}ClGeN_2.0.60\ CH_2Cl_2$) C 51.21, H 7.90, N 6.68; MS $C_{18}H_{33}ClGeN_2$ Calcd.: M^+ = 386; Found: *m/e* 351 (M^+ - Cl).

C, N, N'-[2,6-Bis(Dimethylaminomethyl)-4-(1,1-dimethylethyl)phenyl]-[4,4'-bis (1,1-dimethylethyl)-2,2'-biphenyl]germanium chloride (6). 2,6-Bis(dimethylaminomethyl)-4-(1,1-dimethylethyl)bromobenzene (0.30 g, 0.0009 mol) was dissolved in dry THF in a 25 mL 3-neck round-bottomed flask equipped with magnetic stirrer addition funnel and under inert atmosphere. n-BuLi (0.06 g, 0.0009 mol, 0.57 mL of 1.6 M soln. in hexane) was added dropwise to the solution and the resulting mixture was stirred for 1 h. The solution was then added dropwise to a stirred solution of 2,7-bis(1,1-dimethylethyl)-9,9-dichlorogermafluorene (0.37 g, 0.0009 mol) in THF at RT. White solid product precipitated immediately. The reaction mixture was stirred for 4 h at RT. The solid was isolated by filtration and crystallized from DMSO to yield colorless crystals (0.41 g, 0.0007 mol, 73%). m.p. 268 - 270°C. ^{1}H NMR (acetone-*d6*) δ 8.14 (d, 2H, J = 8.24 Hz), 8.07 (d, 2H, J = 2.14 Hz), 7.69 (dd, 2H, J_1 = 8.24 Hz, J_2 = 2.14 Hz), 7.60 (s, 2H), 4.21 (s, 4H), 2.17 (s, 12H), 1.42 (s, 9H), 1.35 (s, 18H); ^{13}C NMR (acetone-*d6*) δ 198.5, 197.7, 158.2, 152.9, 144.5, 142.6, 132.0, 129.6, 124.0, 123.2, 63.6, 46.8, 36.0, 35.6, 31.7, 31.5; Elem. Analysis: Calcd. ($C_{36}H_{51}ClGeN_2.H_2O$) C 67.78, H 8.37, N 4.39; Found ($C_{36}H_{51}ClGeN_2.H_2O$) C 67.51, H 8.16, N 4.08; MS $C_{36}H_{51}ClGeN_2$ Calcd.: M^+ = 620; Found: *m/e* 585 (M^+ - Cl).

2,6-Bis(Methylaminomethyl)-4-(1,1-dimethylethyl)bromobenzene (14). 2,6-bis(bromomethyl)-4-(1,1-dimethylethyl)bromobenzene (3.00 g, 0.0075 mol) was dissolved in THF (25 mL). Methylamine (9.34 g, 0.3008 mol, 26.0 mL of 40% soln. in water) was added to the solution and the resulting mixture heated at reflux for 4 h. The layers were separated. The organic layer was washed with water and dried over $MgSO_4$. THF was removed under vacuum leaving a yellow oil (1.92 g, 0.0064 mol, 84%) used for the next step without further purification. ^1H NMR (benzene-d_6) δ 7.45 (s, 2H), 3.78 (s, 4H), 2.24 (s, 6H), 1.25 (s, 9H), 0.98 (s, 2H); MS *m/e* (relative intensity) 300 (2.6, $(M + 2)^+$), 299 (13.5, $(M + 1)^+$), 298 (3.1, M^+), 297 (16.1, $(M - 1)^+$), 271 (89.1), 269 (100.0), 240 (47.7), 225 (52.3), 188 (70.0), 161 (28.0), 132 (34.7), 57 (17.6).

2,6-Bis[Methyl(acetyl-*d*3)aminomethyl]-4-(1,1-dimethylethyl) bromobenzene (15). Compound **6** (2.20 g, 0.0074 mol) was dissolved in 30 mL of dry methylene chloride in a 100 mL 3-neck round-bottomed flask equipped with magnetic stirrer, addition funnel and under nitrogen atmosphere. Triethylamine (1.49 g, 0.0147 mol, 2.05 mL) was added to the solution. Acetylchloride-*d*3 (1.20 g, 0.0147 mol, 1.05 mL) in 20 mL of dry methylene chloride was added dropwise over 10 min. The resulting mixture was stirred for 4 h at room temperature, then added to an equal volume of water, the organic layer was separated and dried over $MgSO_4$. The solvent was removed under vacuum leaving a yellow oily material (2.53 g, 0.0065 mol, 89%) which was used directly for the next step. ^1H NMR (benzene-d_6) δ 7.10 (m, 2H), 4.43 (m, 4H), 2.53 (m, 6H), 1.15 (m, 9H); MS *m/e* (relative intensity) 309 (100.0, $(M - Br)^+$), 265 (38.3), 175 (27.5), 59 (38.9).

2,6-Bis[Methyl(ethyl-2,2,2-*d*3)aminomethyl]-4-(1,1-dimethylethyl) bromobenzene (16). Compound **7** (2.53 g, 0.0065 mol) was dissolved in anhydrous THF and transferred into a 100 mL 3-neck flask equipped with addition funnel, reflux condenser and under inert atmosphere. BH_3.THF (21.70 mL, 0.0217 mol, 1 M solution in THF) was added dropwise at 0 - 5°C. The resulting solution was stirred for 10 h at 60°C and 12h at room temperature. 6N HCl (10 mL) was added dropwise. The mixture was heated to reflux and THF distilled at normal pressure. A small amount of water was added followed by extraction with ether (2 x 20 mL). The layers were separated and a concentrated solution of KOH added to the aqueous layer until alkaline reaction (pH = 12 - 13). The mixture was extracted with ether (2 x 50 mL). The combined organic layers were dried over $MgSO_4$. Solvent was removed under reduced pressure to produce a heavy yellow oil (1.70 g, 0.0047 mol, 72%). ^1H NMR (benzene-d_6) δ 7.69 (s, 2H), 3.67 (s, 4H), 2.36 (s, 4H), 2.16 (s, 6H), 1.30 (s, 9H); ^{13}C NMR (benzene-d_6) δ 149.8, 139.9, 126.4, 123.7, 62.4, 51.6, 41.9, 34.6, 31.4; ^2H NMR (CCl_4) δ 1.08 (s); MS *m/e* (relative intensity) 361 (1.0, $(M + 1)^+$), 359 (1.0, $(M - 1)^+$), 344 (27.3), 342 (28.3), 302 (34.5), 301 (37.1), 300 (41.8), 299 (33.0), 241 (65.5), 239 (68.6), 162 (25.8), 75 (100.0), 50 (19.6).

2,6 - Bis[Methyl(ethyl-2,2,2-*d*3)aminomethyl]-4-(1,1-dimethylethyl) phenyllithium (2). Compound **8** (0.60 g, 0.0017 mol) was dissolved in dry THF in a 25 mL 3-neck round-bottomed flask equipped with magnetic stirrer, addition funnel and under inert atmosphere. n-BuLi (1.04 mL, 0.0017 mol, 1.6 M solution in hexane) was added dropwise at RT. The resulting solution was stirred for 1 h. An aliquot quenched with D_2O showed more than 95% incorporation of deuterium according to the ^1H NMR spectrum. ^1H NMR (chloroform-*d*) δ 7.20 (s, 2H), 3.48 (s, 4H), 2.41 (s, 4H), 2.19 (s, 6H), 1.32 (s, 9H).

C,N,N'-[2,6-Bis[Methyl(ethyl-2,2,2-*d*3)aminomethyl]-4-(1,1-dimethylethyl)phenyl]dimethylgermanium chloride (7). A solution of **2** in THF prepared from **1 6** (0.60 g, 0.0017 mol) and n-BuLi (1.04 mL, 0.0017 mol) was added dropwise to a solution of dimethylgermanium dichloride (0.30 g, 0.0017 mol, 0.20 mL) in THF at RT under nitrogen atmosphere. The mixture was stirred for 4h and the white precipitation was separated by vacuum filtration. The solid material was further crystallized from CH_2Cl_2 to yield 0.40 g (0.0009 mol, 57%) of colorless crystals. m.p. 258-260°C. ^1H NMR (D_2O) δ 7.27 (s, 2H), 3.73 (s, 4H), 2.81 (s, 4H), 2.14 (s, 6H), 1.18 (s, 9H), 0.85 (s, 6H); ^{13}C NMR (methanol-d_4) δ 157.6, 143.6, 128.6, 123.8, 62.5, 53.0, 41.4, 36.0, 31.7, 9.5, -0.7; ^2H NMR (methanol) δ 1.30 (s); Elem. Analysis: Calcd. ($C_{20}H_{37}ClGeN_2$.0.55 CH_2Cl_2)

C 53.63, H 8.35, N 6.09; Found ($C_{20}H_{37}ClGeN_2.0.55\ CH_2Cl_2$) C 52.38, H 8.24, N 6.04; MS $C_{20}H_{31}ClD_6GeN_2$ Calcd.: M^+ = 420; Found: *m/z* 385 (M^+ - Cl).

Crystal data of 7. A clear prism crystal of $C_{21}H_{39}Cl_3GeN_2$ ($C_{20}H_{37}ClGeN_2.CH_2Cl_2$) having approximate dimensions of 0.700 x 0.300 x 0.300 mm was mounted on a glass fiber. All measurements were made on a Rigaku AFC6S diffractometer with graphite monochromatic Mo Kα radiation. Cell constants and orientation matrix for data collection, obtained from a least-squares refinement using the angles of 24 carefully centered reflections in the range $34.64 < 2\theta < 36.26°$ corresponded to a monoclinic cell with these dimensions: a = 9.96 (6) Å, b = 24.47 (8) Å, c = 10.71 (7) Å, V = 2415 (2) Å, β = 112.4 (4)°. For Z = 4 and F.W. = 498.50, the calculated density is 1.371 g/cm^3. Based on packing considerations, statistical analysis of the intensity distribution and the successful solution and refinement of the structure, the space group was determined to be $P2_1/n$ (#14). The data were collected at a temperature of -80 ± 1°C using the ω scan technique to a maximum 2θ value of 50.7°. Omega scans of several intense reflections, made prior to data collection, had an average width at half-height of 0.28° with a take-off angle of 6.0°. Scans of (1.34 + 0.30 tan θ)° were made at a speed of 8.0°/min (in omega). Weak reflections ($I < 10.0\ \sigma(I)$) were rescanned (up to 5 rescans) and counts were accumulated to assure good statistics. Stationary background counts were recorded on each side of the reflection. The ratio of peak counting to background counting time was 2:1. The diameter of the incident beam collimator was 0.5 mm. The crystal to detector distance was 200.0 mm.

Of the 4671 reflections which were collected, 4407 were unique (R_{int} = 0.113). Intensities of three representative reflections measured after every 150 reflections declined by -3.50%. A linear correction was applied to account for this phenomenon. The linear absorption coefficient for Mo Kα is 16.0 cm^{-1}. An empirical absorption correction, based on azimuthal scans of several reflections, was applied giving transmission factors from 0.85 to 1.00. Data were corrected for Lorentz and polarization effects.

Solution and refinement of the structure of 7. The structure was solved by direct methods[17, 18]. The non-hydrogen atoms were refined anisotropically. The final cycle of full-matrix least-squares refinement[19] was based on 2564 observed reflections ($I > 3.00\ \sigma(I)$) and 208 variable positional and thermal parameters and converged (largest parameter shift was 0.35 times its esd) with unweighted and weighted agreement factors of: R = 0.093 and R_w = 0.140. The standard deviation of an observation of unit weight[20] was 4.84. The weighting scheme was based on counting statistics and included a factor (ρ = 0.03) to downweight the intense reflections. Plots of $\Sigma\ w\ (|F_o| - |F_c|)^2$ versus |Fo|, reflection order in data collection, sin θ/λ, and various classes of indices showed no unusual trends. The maximum and minimum peaks on the final difference density Fourier map corresponded to 1.16 and -1.04 e$^-$/Å^3, respectively. Neutral atom scattering factors were taken from Cromer and Waber[21]. Anomalous dispersion effects were included in F_{calc}[22]; the values for Δf' and Δf" were those of Cromer[23]. All calculations were performed using the TEXSAN[24] crystallographic software package of Molecular Structure Corporation.

RESULTS

Synthesis and characterization of compounds 3, 4, 5 and 6. These compounds are prepared in a moderate to high yield by using the synthetic sequence outlined in Scheme 1. The final materials are insoluble in THF and precipitate from the solution with the progress of the reaction. Solubility tests are consistent with an ionic nature of the compounds. Solubility in water is dependent on the size of the hydrocarbon substituents as manifest by the significantly lower solubility of **6** in comparison to **5**. All compounds are well soluble in alcohols. The solubility in polar aprotic and halogenated solvents seems to be dependent on the central atom and increases upon transition from silicon to germanium. The melting points of all compounds are high, around and above 200°C. Thus, the melting points and the solubility trends, combined with positive $AgNO_3$ tests, are indicative for an ionic nature of these compounds. Corriu and coworkers performed conductivity measurements on similar structures which also confirmed

the ionic nature of the studied compounds.[13a] In the solid state the ionic nature of the compounds, with a chloride anion as a counterpart, is supported by evidence from the X-ray crystal structures of both compound **3** and compound **7**.

Synthesis of the ^{15}N-enriched analog of compound 3 (compound 3*). Compound **3*** was prepared from the brominated precursor **12*** according to the previously discussed synthetic procedure of Scheme 1. However, compound **12*** was prepared by a substantially modified sequence outlined in Scheme 2. The main requirement was to find a more efficient way of introducing the dimethylamino moiety in the molecule. The procedure used for the synthesis of **12** utilizes a water solution of dimethylamine but a large excess is necessary to drive the reaction to completion.[25, 26] Therefore the substitution at benzylic carbon was replaced with a substitution at an acyclic carbon atom in the form of the corresponding acyl chloride. The first step of the modified synthetic sequence is the introduction of bromine which proceeds in high yield under ordinary conditions for aromatic electrophilic substitutions.[27] Compound **8** is then oxidized to the corresponding dicarboxylic acid with $KMnO_4$ in a 1:1 water/*t*-butanol mixture. The conversion of the diacid **9** to the dichloride **10** is achieved with PCl_5 in the solid phase at elevated temperatures. Compound **10** is reacted with the isotopically enriched ammonium salt in the presence of triethylamine according to a slight modification of the original procedure.[28] At these conditions, the triethylamine acts as a base and abstracts a proton from the ammonium salt liberating dimethylamine which reacts with the acid chloride to yield compound **11**. The final step is a reduction of **11** to give **12*** with a borane/tetrahydrofuran complex.[29, 30]

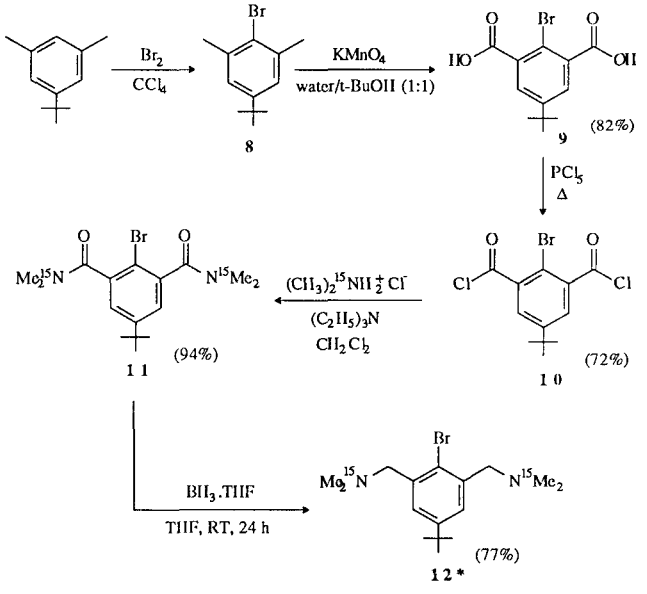

Scheme 2. Preparation of an ^{15}N-labeled precursor for tridentate ligand **1**.

Synthesis of compound 7. Compound **7** is prepared according to the synthetic sequence outlined in Scheme 1 from the new tridentate ligand **2**. The precursor for **2** was synthesized according to the sequence outlined in Scheme 3. The synthesis utilizes the tribromide **7**[31, 32] which is subjected to a reaction of nucleophilic substitution with methylamine in nonhomogenuous conditions.[25] The resulting bisamine **14** is converted to the bisamide **15** upon reaction with acetylchloride-*d*3. Compound **15** is reduced with borane/THF complex to yield the brominated precursor **16**,[29] which is converted, upon reaction with n-BuLi, to the new tridentate ligand **2**. Ligand **2** is reacted with $(CH_3)_2GeCl_2$ at room temperature in THF to give the target compound **7**.

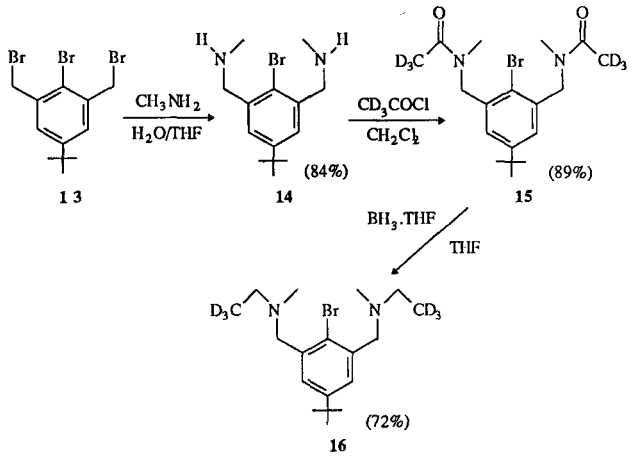

Scheme 3. *Synthetic sequence for the preparation of the precursor to tridentate ligand* **2**.

^{15}N NMR data for compound 3. The variable temperature ^{1}H and ^{13}C NMR profiles of compound **3** were described in an earlier work. All data are rigorously consistent with the existence of asymmetrical structures in solution. The ^{15}N studies provide further support for this hypothesis. The ^{15}N spectra at 315 K and 200 K in methanol-*d*4 are presented in Figure 3. As seen from the figure, at higher temperatures, in conditions of fast exchange, the spectrum is an averaged signal for both nitrogen atoms at 40.35 ppm. At lower temperatures, with the exchange sufficiently slow, the two nitrogen signals are clearly distinguished at 47.70 ppm and 35.92 ppm.

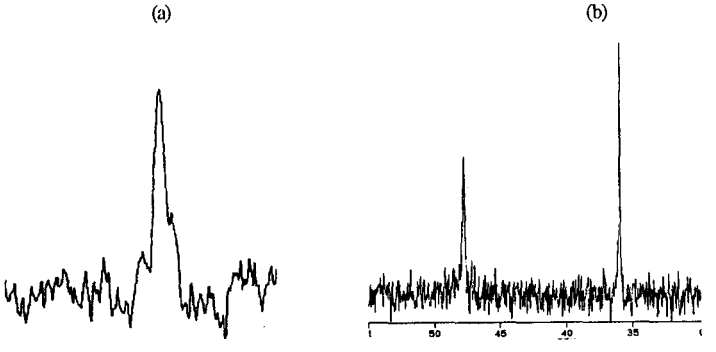

Figure 3. ^{15}N NMR spectrum of compound **3** at (a) 315 K and (b) 200 K in methanol-*d*4.

NMR properties of compound 4. Although very similar to compound **3**, compound **4** provides more structural information due to the lower symmetry of the pattern of substitution around the central silicon atom. If the real state in solution is a pair of asymmetrical structures, then in each of these structures there would be a silicon chiral center present. The chiral silicon environment causes the generation of diastereotopic centers, the two methylene carbon atoms as well as the quaternary nitrogen bound to silicon as indicated in structure **4a**. The spectral properties of NMR active nuclei, connected to a particular diastereotopic center, are different in general.

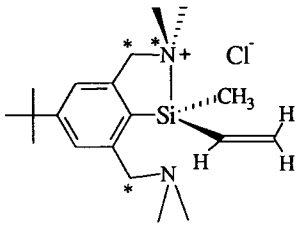

4a

The variable temperature ^{1}H NMR profile of **4** in methanol-*d4* is shown in Figure 4. At 298 K the spectrum contains a well defined singlet for the two aromatic protons at 7.39 ppm. The vinyl protons exhibit separate signals at 6.26 ppm, 6.16 ppm and 5.83 ppm respectively. There are two broad singlets in the spectrum, one for the N-methylene and one for the N-methyl protons at 3.95 and 2.44 ppm. The signals for the protons belonging to the tertiary butyl group and the Si-methyl groups are at 1.34 and 0.51 ppm respectively. The substantial broadening of the signals for the N-methyl and the N-methylene groups is a good indication for a dynamic process in solution. As expected, with decrease of the temperature, these averaged signals reach coalescence points. For the N-methylene protons this occurs at T_C = 258 K leading to the generation of four doublets of equal intensity at 4.52, 4.23, 3.81 and 3.15 ppm, corresponding to the four different hydrogen atoms. The doublet pattern is due to the geminal spin coupling. More interesting is the behavior of the N-methyl resonance. The averaged signal for all methyl groups generates a pair of broad singlets of equal intensity at 265 K. The peak at lower field reaches in its turn a coalescence point at 253 K giving, upon further reduction of the temperature, a pair of singlets with intensity ratio 1:1 at δ = 2.98 ppm and δ = 2.81 ppm. The changes in the aliphatic region are accompanied by changes in the aromatic region as well, where the singlet for the two aromatic protons reaches a point of coalescence at 238 K and also generates a pair of singlets at 7.50 and 7.36 ppm. At 213 K (Figure 4b) the spectrum contains two singlets for the aromatic protons, four doublets for the N-methylene protons and three singlets for the N-methyl groups with ratio 1:1:2 (in upfield direction). Further decrease of the temperature causes additional broadening of the upfield N-methyl resonance with double intensity located at δ = 2.00 ppm.

At 203 K it is at a coalescence point and further lowering of the temperature leads to the generation of another pair of singlets of equal intensity at 2.22 and 1.78 ppm (Figure 4c). At very low temperatures we observe species in which the second nitrogen atom is also a diastereotopic center, i.e. it is also coordinated to silicon. The species retains its asymmetrical structure as evidenced by the different shape of the two pairs of singlets in the N-methyl region of the spectrum in Figure 4c.

The ^{13}C NMR spectrum at 298 K exhibits averaged singlets for the N-methylene and the N-methyl carbon atoms at 65.06 and 43.93 ppm respectively. At 193 K the spectrum contains two singlets for the N-methylene groups at 65.09 and 63.41 ppm and four broad singlets for the N-methyl carbons at 46.03, 44.11, 41.12 and 40.08 ppm. The number of singlets for the aromatic carbon atoms increases from four to six in accordance with a lower symmetry of the species in solution.

Kinetic parameters from NMR studies of compound 4. The variable temperature NMR profile of compound **4** offers several coalescence temperatures and allows for the construction of Arrhenius and Eyring plots and elucidation of activation parameters.[33] The results are listed in Table 1. The Eyring plot is presented in Figure 5. The good straight line fit (R = 0.99) is an evidence that the coalescence temperatures all pertain to the same dynamic equilibrium.

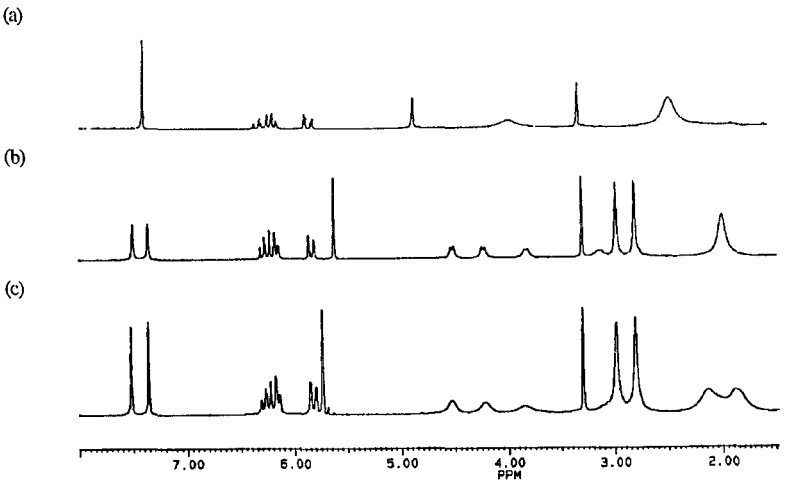

Figure 4. Selected region from the ^1H NMR spectrum of compound **4** at (a) 298 K, (b) 213 K and (c) 193 K in methanol-d_4.

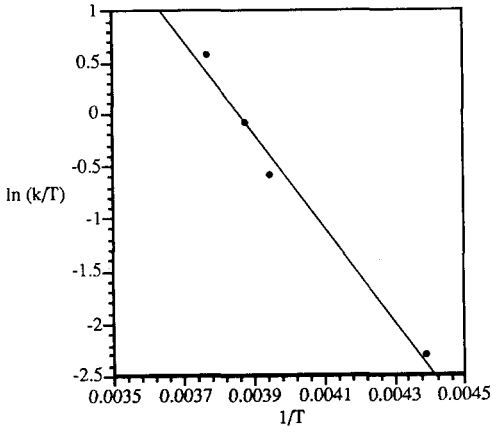

Figure 5. Eyring plot for compound **4** in methanol-d_4.

Table 1. Kinetic Parameters from Variable Temperature NMR Studies of Compound **4**

solvent	ΔG^* [kJ/mol]	ΔH^* [kJ/mol]	ΔS^* [J/mol.K]	E_a [kJ/mol]	ln A
CD_3OD	51.0	37.2	- 54	39.8	24.1
C_2H_5OD	53.8	-	-	-	-

Table 2. Experimental Results and Activation Parameters for the Si-N Ring Opening in Compound **4** at low temperatures

Solvent	T_c [K]	$\Delta\nu$ [Hz]	k x 10^2 [s^{-1}]	ΔG_1^* [kJ/mol]
Methanol-d_4	203	105	2.33	39.8
Ethanol-d_6	210	120	2.66	41.0

Information was extracted about the second dynamic process from the low temperature coalescence of the upfield N-methyl resonance. Table 2 presents the experimental results and the activation energies in methanol-d_4 and ethanol-d_6 solutions of compound **4**.

NMR studies of compounds 5 and 6. The ^{1}H NMR spectra of compound **5** in methanol-d_4 at 298 K and 183 K are shown in Figure 6. There is an obvious difference between the NMR behavior of this germanium containing compound, compared to its silicon analog, compound **2**. At room temperature the spectrum contains only well defined, sharp singlets. The spectral pattern is preserved throughout the studied region. The broadening at 183 K of the N-methylene and the N-methyl resonances, at 3.94 ppm and 2.50 ppm respectively, can be partially attributed to the considerable increase of the viscosity of the solution and the concomitant worsening of the homogeneity of the magnetic field, leading to an overall broadening of the signals. It is important to notice that the signal for the aromatic protons is not affected, which means that the dynamic process, leading to the broadening of the N-methyl and the N-methylene peaks, is not identical with the process occurring in the silicon-containing species.

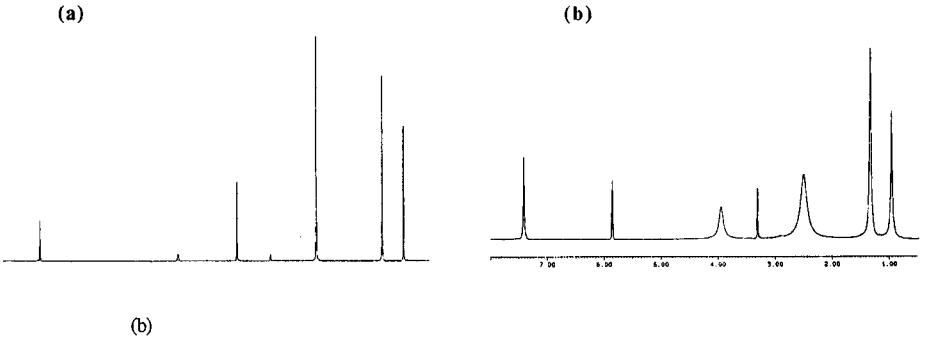

Figure 6. ^{1}H NMR spectrum of compound **5** at (a) 298 K and (b) 183 K in methanol-d_4.

The ^{13}C NMR spectra of **5** do not show any changes of pattern over the studied region 298 K - 183 K and remain consistent with a symmetrical pentavalent structure. The ^{1}H and ^{13}C NMR spectra of **6** are similarly in agreement with the pentavalent structure within the studied temperature interval.

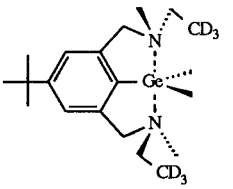

7

NMR studies of compound 7. An ^1H variable temperature NMR profile of compound **7** is shown in Figure 7.

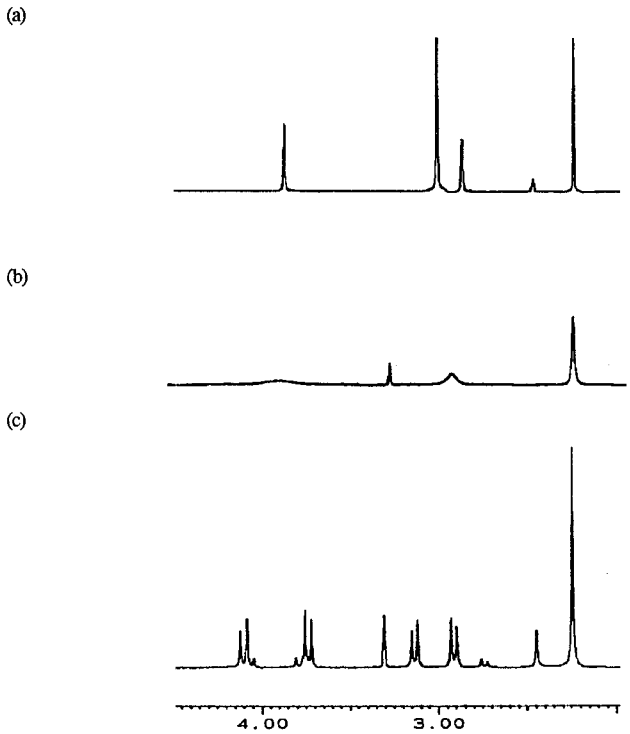

Figure 7. Selected region from the ^1H NMR spectrum of compound **7** at (a) 343 K in DMSO-d_6, (b) 298 K in methanol-d_4 and (c) 223 K in methanol-d_4.

Figure 7b is the spectrum of **7** in methanol-d_4 at 298 K. It contains a singlet for the aromatic protons at 7.40 ppm, a broad singlet for the benzylic N-methylene protons at 3.91 ppm, a broad singlet for the ethyl N-methylene groups at 2.97 ppm, a broad singlet for the N-methyl groups at 2.30 ppm, a singlet for the protons of the tertiary butyl group at 1.33 ppm and a singlet for the Ge-methyl groups at 1.00 ppm. Figure 7c is the spectrum of **7** in methanol-d_4 at 223 K. As seen from the figure, changes occur only in the region of the signals for groups attached to the nitrogen atoms. It is quite evident that in this region there are two sets of signals, identical in pattern but very different in intensity. Each set consists of two AB pattern multiplets for the benzylic and ethyl N-methylene groups respectively, and a singlet in the N-methyl region. The intensity ratio is 8:1.

The behavior of the system is similar in other solvents. In DMSO-d_6 and in methylene chloride-d_2 the spectra at room temperature exhibit similar broadening of selected peaks and the coalescence temperatures are 300 K for methylene chloride and 305 K for DMSO. Figure 7a is the spectrum of **7** in DMSO-d_6 at 343 K. Noticeable is the considerable sharpening of the N-methylene and N-methyl signals. NMR observations allow quantitative conclusions about the energy barrier ΔG^*. In methanol-d_4 the coalescence temperature is 288 K with separation of the peaks $\Delta\nu$ = 54 Hz. Such separation corresponds to an unimolecular rate constant of 119 s^{-1}, leading to a Gibbs free energy barrier of 58.9 kJ/mol (14.1 kcal/mol).[33]

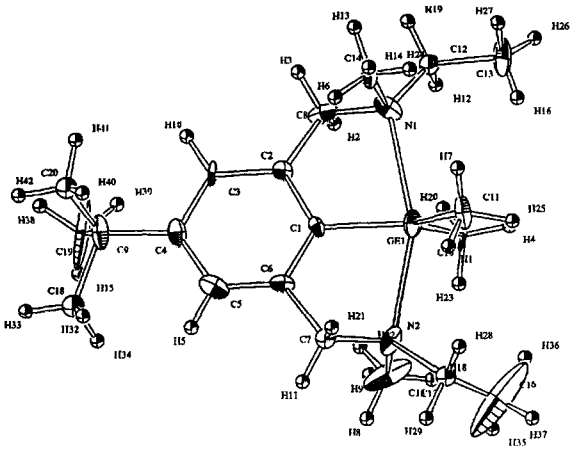

Figure 8. An ORTEP drawing of the cationic part of compound **7**. Ellipsoids drawn with 30% probability.

X-ray crystal structure of compound 7. Figure 8 shows an ORTEP drawing of the crystal structure of the cationic part of compound **7**. The ellipsoids are drawn with 30% probability. Selected bond lengths and bond angles are given in Table 3. The geometry around the central germanium atom is a distorted trigonal bipyramid (TBP). The germanium-carbon bonds are within the expected range, all three carbon ligands are located in the equatorial plane with proper values for the C - Ge - C bond angles. The Ge - N distances are essentially equal, with values of 2.31 Å and 2.36 Å indicating that compound **7** possesses a symmetrical structure in solid state. The N - Ge - N angle is distorted from the perfect 180° with a real value of 158° at this level of refinement. The distortion is in a direction opposite to the Berry pseudorotation coordinate and the immediate surrounding of the germanium atom acquires a C_{2v} symmetry. The five-membered rings are not planar. The only flexible point in either ring is located at the nitrogen atom, which is shifted from the plane determined by the other four atoms of the ring. The distortion is in opposite direction for the two nitrogen atoms relative to the plane of the benzene ring and the overall environment around the central germanium atom resembles closely an S_N2-like transition state with a backside attack of the incoming nucleophile.

Table 3. Selected Bond Distances [Å] and Bond Angles [Degrees] from X-Ray Structural Analysis of Compound **7**

Ge - C1	1.88 (1)
Ge - C10	1.91(2)
Ge - C11	1.97(2)
Ge - N1	2.31(2)
Ge - N2	2.36(2)
C1 - Ge - N1	79.8(5)
C1 - Ge - N2	78.2(5)
N1 - Ge - N2	158.0(4)
C10 - Ge - C11	119.0(7)

DISCUSSION

The structure of compound 4. There are two different ways to account for the ionic structure of compounds **3** and **4**. One utilizes the idea of dynamic equilibrium between tetravalent forms, the other is based on the hypothesis for a stable hypervalent species. Observations for compound **4**, in analogy with the earlier results for **3**, unambiguously demonstrate a dynamic process in solution. This is a good argument in favor of the tetravalent structures **4a** and **4a'**. However, there is an alternative explanation, which has been successfully employed in a variety of silicon-containing, hypercoordinated and hypervalent systems.[5d,e, 34] It is based on the interconversion of hypervalent forms via a process not involving breaking and remaking of bonds, such as the Berry pseudorotation or the turnstile rotation.[35, 36] Three such forms for compound **4** are shown in Scheme 4. In form **4b** the two nitrogen atoms occupy the axial positions of the trigonal bipyramid, while the carbon ligands are located at the equatorial sites. In the form **4c**, the axial positions are occupied by the Si-methyl group and the aromatic carbon atom. The two nitrogen atoms are equatorial ligands. In form **4d** the axial sites are occupied by the carbon atom from the vinyl group and the aromatic carbon.

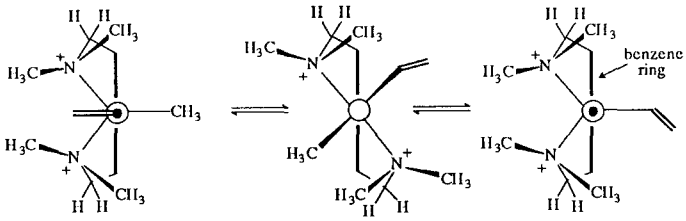

4d **4b** **4c**

Scheme 4. Pseudorotational forms arising due to a hypothetical pentavalent silicon center in compound **4**.

All three forms possess a high degree of symmetry and within each of them the aromatic hydrogen atoms are equivalent. Ideally, in conditions of slow exchange, the ^{1}H NMR spectrum would be expected to show three singlets in the aromatic region, but taking in account the similarity of forms **4c** and **4d**, and the remoteness of the aromatic sites from the center of inversion, some of the signals may coincide. In forms **4c** and **4d**, however, the nature of the groups attached to silicon is different. In **4c** for example, the Si-methyl group is occupying an axial position whereas in **4d** the same group is at an equatorial site. Overall, at least two (in the ideal case three) signals for the Si-methyl and the vinyl group would be expected in the NMR spectra or at least broadening of the corresponding signals. The fact is that neither in the proton nor in the carbon spectra is this observed at any temperature within the studied range. The lower symmetry of **4c** and **4d** would also cause inequivalency of the N-methyl groups and the N-methylene hydrogen atoms within each structure, and an overall complicated NMR pattern would be expected. The actual pattern, as demonstrated in Figures 4b and 4c is simple and well resolved. Our conclusion is that the accumulated NMR evidence does not support the idea of equilibrium between hypervalent forms in solution. The experimental data are, however, consistent with the presence of the asymmetrical, tetravalent forms.

In our previous report we discussed briefly the mechanism of identity exchange in compound **3**. The considerable solvent effect upon transition from methanol to chloroform is indicative for a process with a charge delocalized transition state, leading to increase of the reaction rate upon reduction of the solvent polarity, i.e. an S_N2 like mechanism. An associative rate-determining step is also supported by the considerable negative entropy of activation $\Delta S^* = -54$ J/mol.K in methanol-*d*$_4$ for compound **4**.[37, 38]

It was pointed out that at very low temperatures (below 203 K in methanol-d_4) the upfield N-methyl signal at 2.00 ppm, in the ^{1}H NMR spectrum of **4**, generates a pair of singlets of equal intensity. As mentioned, it is an evidence for the presence of another, distinct species in solution, structure **4e**, in which the second nitrogen atom is also coordinated to the silicon center.

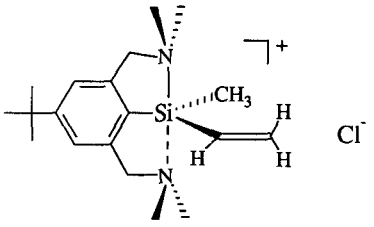

4e

Form **4e** is the most stable since it is the one observed at the low temperature limit. Therefore, in solution of **4** there are four asymmetric forms. Two of them are the open, tetravalent forms, the other two are forms with a partial bonding to the second nitrogen atom. The closed forms are related to the open via an energy barrier ΔG_1^* of about 40 kJ/mol in deuterated alcohols, and are related between themselves via a central barrier ΔG^* which is slightly more than 50 kJ/mol.

The proposed energy profile for the identity exchange in compound **4** is shown in Figure 9. Such profiles are characteristic for S_N2 reactions at carbon in the gas phase.[39] The global minima arise due to the formation of the so called nucleophile-substrate association complexes. In solution, especially in polar protic solvents, the magnitude of these minima is largely reduced leading to their virtual disappearance.[40]

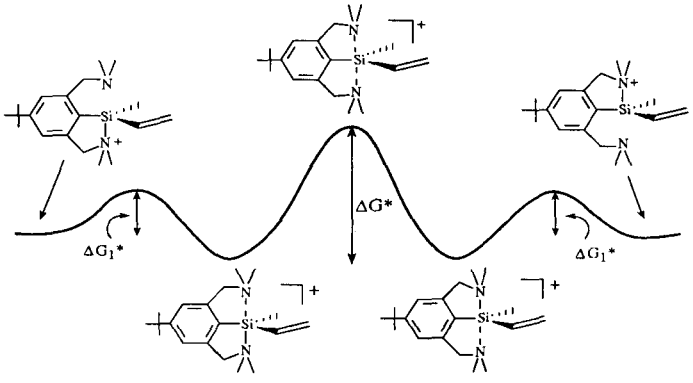

Figure 9. Two-dimensional potential energy surface for the identity exchange in compound **4**.

The structure of compounds 5 and 6. These two germanium compounds are prepared by means of the same tridentate ligand **1**. Compound **5** is the germanium-containing analog of compound **3**. Compound **6** is particularly interesting from a structural point of view since it incorporates a tridentate and a bidentate ligand at a single center of hypercoordination.

As NMR studies demonstrate, the behavior of **5** and **6** in solution is significantly different in comparison to the silicon species. Down to 183 K, there is no change in the spectral pattern. This could mean either that the identity exchange reaction is very fast or that they exist in solution as stable hypervalent structures and thus their NMR spectra do not change with temperature.

Particular attention attends the fact that the broadening is restricted only to the N-methyl and N-methylene groups. The aromatic signal is not affected. It must be a process which does not destroy the overall symmetry in the molecule and exerts only a local effect on the groups attached to nitrogen. A good explanation would be the dynamic process of pseudorotation of the five-membered ring via envelope-type vibrations as shown in Figure 10.[41] The only flexible point is the nitrogen atom and distortions at this point, above and below the plane determined by the other four atoms, would explain the broadening of the N-methylene and the N-methyl groups. In the case of assigning structures to both **5** and **6**, caution must be exercised, because the available facts agree with the presence of hypervalent structures in solution, but they need not rigorously exclude equilibrium between open, tetravalent forms.

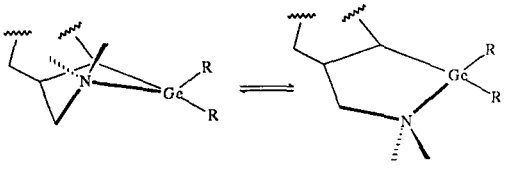

Figure 10. Pseudorotational envelope vibrations in the five-membered ring.

The structure of compound 7. Compound **7** is derived on the basis of a different tridentate ligand, one with a lower symmetry of substitution at the nitrogen atoms. The replacement of one of the methyl groups with a 2,2,2-trideuteroethyl group at each nitrogen center has important consequences. Upon bonding with germanium the nitrogen atom becomes a chiral center. Therefore, presence of the tetravalent forms in solution, as is the case with the silicon-containing materials, would lead to a pair of enantiomers, indistinguishable by NMR. However, if both nitrogen atoms are connected to germanium, that would lead to the generation of two chiral centers in the molecule and hence to the formation of two diastereomers, whose NMR properties are different in general and whose distribution is not required to be 1:1.

The broad singlets at 298 K certainly indicate a dynamic process. Indeed, the behavior of the system around and above room temperatures is consistent with the presence of the open tetravalent forms in equilibrium. The spectrum at 223 K is not, however, in agreement with such hypothesis. The two equivalent in pattern but different in intensity sets of signals in the (N-methylene + N-methyl) region are suggestive for the presence of two diastereomers. Therefore, an energy surface with a low laying intermediate is proposed for the dynamic process in solution of **7** (Figure 11). The intermediate is the pentavalent symmetrical structure and its energy is actually lower compared to the open forms.[2, 9] The energy barrier is sufficiently small so that above room temperature it is overcome and a certain amount of the open forms **7"** is generated. The open forms have one of the dialkylaminomethyl moieties free and therefore rotation around single bonds and inversion at the nitrogen become possible. This process leads to a loss of stereochemistry and broadening of the peaks of groups attached to the nitrogen atoms. As the temperature is decreased, the rate of the transition **7'** ⟶ **7"** is reduced and eventually the molecule is trapped inside the potential well. The collapse to **7'** leads to the formation of two diastereomers in a ratio dependent on their relative energies.

The X-ray studies of **7** reveal a symmetrical, pentavalent structure with a C_{2v} geometry around the germanium atom. The distortion of the N - Ge - N angle is very important in our opinion, as one significant cause for the structural difference between the studied silicon and germanium molecules. It is also important to remark here that the X-ray information may be in many instances insufficient for correct conclusions about the nature of certain species. Thus, for compound **7** it shows a symmetrical and hypervalent structure, but, as demonstrated, this is the prevailing structure in solution only at low temperatures. At higher temperatures, solution studies yield a more complex exchange process. Therefore hypercoordination and hypervalency in the condensed phase may not be necessarily exhibited in solution.

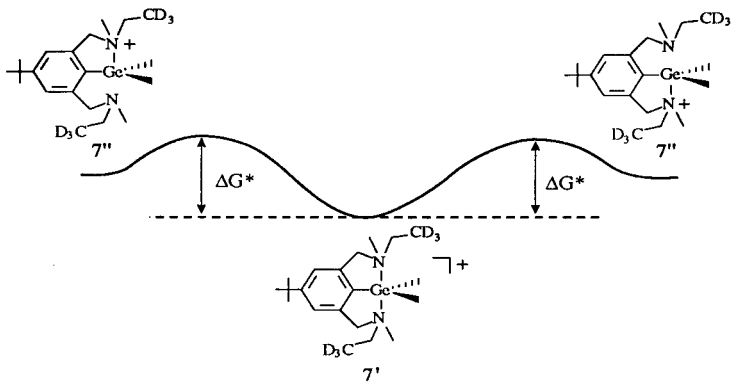

Figure 11. Two-dimensional energy surface for the intramolecular exchange in **7**.

Comparison between the silicon and germanium molecules. A detailed investigation of their solution behavior has shown that the silicon-containing molecules (Compounds **3** and **4**) are asymmetrical, with loose or no bonding of the second nitrogen atom to the silicon center. On the other hand, the germanium compounds exhibit properties consistent with a hypervalent structure. For some of them (compounds **5** and **6**) the solution NMR behavior is uniform throughout the studied temperature range and consistent with hypervalent symmetrical structure involving an equal extent of bonding from both nitrogen atoms. One of the studied compounds (Compound **7**) demonstrates an interesting NMR profile corresponding to a different type of potential energy surface with a stable "intermediate". The "intermediate" is in fact the hypervalent structure and is lower in energy compared to the open, tetravalent forms. Solid state studies (X-ray analysis) have also revealed a hypervalent symmetrical structure for this compound. An important question then is: What are the reasons for such a considerable difference between these two classes of compounds? Germanium exhibits an obvious tendency for hypervalent bonding while the silicon compounds remain tetravalent.

An answer can be found by relating the known experimental results to the contemporary theoretical models. The following facts have to be considered:

1. As revealed by the X-ray data and semiempirical calculations, the axial ligand-central atom-axial ligand angle is less than 180°. Its actual values are about 160° and are predetermined by the properties of the tridentate ligand. The resultant geometry is a distorted TBP and the immediate environment of the central atom determines a C_{2v} instead of D_{3h} symmetry point group. Such geometry is unachievable in the absence of a tridentate ligand. It is in fact a distortion in a direction opposite the Berry pseudorotation coordinate.

2. Semiempirical calculations (AM1, PM3)[42 - 46] of small molecules: SiH_5^-, GeH_5^-, $SiH_3F_2^-$, $GeH_3F_2^-$, with both D_{3h} and C_{2v} symmetries, show a considerable difference in the arrangement of the molecular orbitals on the energy scale. The results for SiH_5^- and GeH_5^- with C_{2v} symmetry are shown in Figure 12. The orbitals of concern are $1B_2$, $3A_1$, $4A_1$ and $2B_2$ for the silicon-containing molecule and $1B_2$, $3A_1$, $5A_1$ and $2B_2$ for the germanium molecule. Comparison with Figure 1 shows that the B_2 orbitals in Figure 12 correspond to the bonding and antibonding orbitals in Figure 1. On nonbonding level the diagram from Figure 1 displays an interaction between a classical Musher-Rundle nonbonding orbital and an antibonding orbital distributed over the central atom and the equatorial substituents. Such interaction leads to the generation of two orbitals as illustrated in Figure 13.

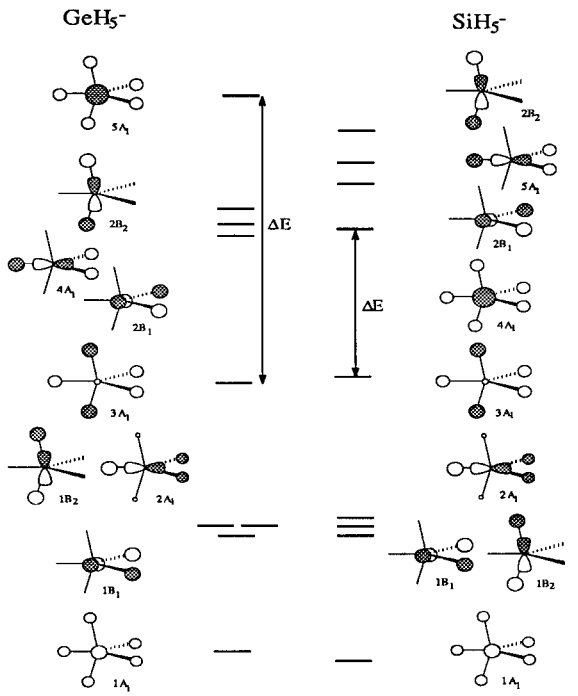

Figure 12. MO correlations for SiH_5^- and GeH_5^- with C_{2v} symmetry.

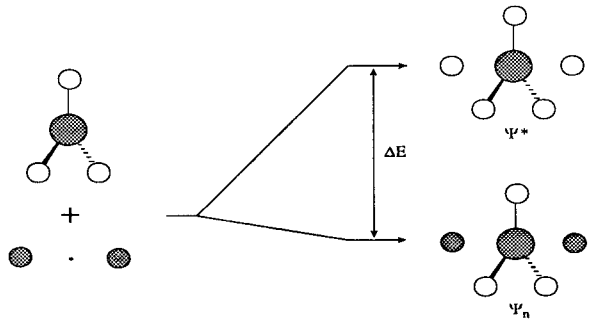

Figure 13. Orbital interaction on nonbonding level in hypervalent molecules.

The resultant orbitals in Figure 13 are the analogs of the $3A_1$ and $4A_1$ (or $3A_1$ and $5A_1$) orbitals for the silicon (germanium) species in Figure 12. The lower energy orbital Ψ_n always remains close to the nonbonding level since the effects of axial and equatorial overlap nearly cancel each other. The second orbital Ψ^*, with strong antibonding interactions, is significantly higher in energy. The separation ΔE depends on the efficiency of overlap between the equatorial fragment antibonding orbital and the orbitals of the axial ligands. Comparison with Figure 12 leads to the conclusion that, for germanium, the overlap is substantially stronger, causing a much greater separation ΔE. This axial-equatorial overlap is essential for the formation and stability of

hypervalent molecules. Therefore, germanium containing molecules have a higher chance of being hypervalent because of the significantly more efficient overlap.

The overlap depicted in Figure 13 is of σ type and will be sensitive to changes in the axial ligand-center-axial ligand angle.[47] It is strongest at an angle of 180° and decreases with any distortion towards bigger or smaller values. The tridentate ligand, however, forces the molecule to adopt a distorted TBP geometry. And with the overlap being initially smaller in the Si-molecule, it is further reduced with this transition from D_{3h} to C_{2v} symmetry, which eventually makes it impossible to form a stable hypervalent structure. The effect of angle reduction is the same in Ge-molecules, but the overlap is initially much stronger and the formation of a hypervalent molecule remains energetically possible.

CONCLUSION

The NMR observations of the studied by us silicon- and germanium-containing species have demonstrated important differences in their solution structures. All the studied systems have proved to be stable isolable compounds with ionic nature. The silicon molecules have exhibited properties consistent with the presence of an intramolecular identity exchange process. The studies have shown, for compound **4**, that unlike the S_N2 reactions at carbon, in the case of silicon the nucleophile-substrate complex is detectable in polar protic solvents and is located at the lowest minimum along the reaction coordinate of the exchange process. This phenomenon can be, at least partially, attributed to the reduced magnitude of the negative entropy of its formation, due to the properties of the tridentate ligand.

The studies of these silicon-containing systems have virtually excluded the presence of pentavalent, symmetrical forms as stable species in solution. The idea of a pseudorotational process of interconversion between hypervalent structures can, in theory, be employed to explain the dynamic NMR phenomena. However, the expected NMR patterns significantly contradict the actual measurements.

The studies of compounds **5** and **6** are incomplete. Although the NMR evidence supports the presence of stable pentavalent and symmetrical species, there remains a finite probability for intramolecular identity exchange. Compound **7** has been studied thoroughly, both in solution and in the solid state. Its solution behavior is a rare example of a *profile with a stable, observable "frozen transition state".*

All studied compounds contain a tridentate ligand incorporated in their structures. The use of tridentate ligands for preparation of hypervalent compounds is beneficial because it fixes to a large extent certain ligand sites around the central atom. Thus it reduces, in magnitude, the entropy of formation of hypervalent molecules by decreasing the negative entropy of association. On the other hand, the tridentate ligand causes distortions from the ideal TBP geometry. Such distortions reduce the efficiency of certain orbital overlaps responsible for the formation of hypervalent structures.

Acknowledgments. This research project was supported by a grant from the National Institute of Health (NIH 5 R01 GM36844-07). The authors are grateful to Markus Vöchler for assistance in the variable temperature NMR measurements and to Dr. Mahesh Patel for valuable assistance in the X-ray studies.

Supplementary Material Available. A listing of atomic coordinates, thermal parameters, complete bond angles and bond lengths from the X-ray structural analysis of compound **7** (9 pages).

Present address: Department of Chemistry, Baker Laboratory, Cornell University, Ithaca, NY 14853-1301.

Present address: Department of Radiology, University of Texas Medical Branch, Galveston, TX 77555-0793.

REFERENCES AND NOTES

1. Benin, V. A.; Martin, J. C.; Willcott, M. R. *Tetrahedron Lett.* **1994**, *35*, 2133.
2. Martin, J. C. *Science* **1983**, *221*, 509.
3. Corriu, R. J. P.; Young, J. C. *The Chemistry of Organic Silicon Compounds*, Editor: S. Patai, Wiley, NY, **1989**, 1241 - 1289, and references therein.
4. Chuit, C.; Corriu, R. J. P.; Reye, C.; Young, J. C. *Chem. Rev.* **1993**, *93*, 1371, and references therein.
5. (a) Forbus, T. R., Jr.; Martin, J. C. *J. Am. Chem. Soc.* **1979**, *101*, 5057. (b) Forbus, T. R., Jr.; Martin, J. C. *Hetroatom Chem.* **1993**, *4*, 113. (c) Forbus, T. R., Jr.; Martin, J. C. *Hetroatom Chem.* **1993**, *4*, 129. (d) Stevenson, W. H., III; Wilson, S.; Martin, J. C.; Farnham, W. B. *J. Am. Chem. Soc.* **1985**, 107, 6340. (e) Stevenson, W. H., III; Martin, J. C. *J. Am. Chem. Soc.* **1985**, 107, 6352.
6. Musher, J. I. *Angew. Chem. Int. Ed. Engl.* **1969**, *8*, 54.
7. Epiotis, N. D. *Lecture Notes in Chemistry* **1983**, *34*, 265.
8. Gimarc, B. M. *Molecular Structure and Bonding. The Qualitative Molecular Orbital Approach*, Academic Press, London, **1979**, 79.
9. Sini, G.; Ohanessian, G.; Hiberty, P. C.; Shaik, S. *J. Am. Chem. Soc.* **1990**, *112*, 1407.
10. Shaik, S.; Duzy, E.; Bartuv, A. *J. Phys. Chem.* **1990**, *94*, 6574.
11. Reed, A. E.; Schleyer, P. v. R. *J. Am. Chem. Soc.* **1990**, *112*, 1434.
12. Koten, G. V.; Jastrzebski, J. T. B. H.; Noltes, J. G.; Spek, A. L.; Schoone, J. C. *J. Organomet. Chem.* **1978**, *148*, 233.
13. (a) Chuit, C.; Corriu, R. J. P.; Mehdi, A.; Reye, C. *Angew. Chem. Int. Ed. Engl.* **1993**, *32*, 1311. (b) Chanhan, M.; Chuit, C.; Corriu, R. J. P.; Reye, C. *Tetrahedron Lett.* **1996**, *37*, 845.
14. Cotton, F. A.; Wilkinson, G. *Advanced Inorganic Chemistry*, 5th Ed., Wiley, New York, **1988**, 266.
15. Freeman, R.; Hill, H. D. W.; Kaptein, R. *J. Magn. Res.* **1972**, *7*, 327.
16. Witanowski, M.; Stefaniak, L.; Webb, G. *Annu. Rep. NMR Spectrosc.* **1991**, *25*, 86.
17. Calabrese, J. C. *Ph. D. Dissertation*, University of Wisconsin - Madison, **1972**.
18. Beurskens, P. T. *Technical Report*, Crystallography Laboratory, Toernooiveld, 6525 Ed., Nijmegen Netherlands.
19. Least-Squares Function Minimized: S w $(|F_O| - |F_C|)^2$, Where w = $4F_O^2/s^2(F_O^2)$, $s^2(F_O^2) = [S^2 (C + R^2B) + (rF_O^2)^2]/Lp2$, S = Scan Rate, C = Total Integrated Peak Count, R = Ratio of Scan Time to Background Counting Time, B = Total Background Count, Lp = Lorentz-Polarization Factor, r = r-Factor.
20. Standard Deviation of an Observation of Unit Weight: $[Sw (|F_O| - |F_C|)^2/(N_O - N_V)]^{1/2}$, Where N_O = Number of Observations, N_V = Number of Variables.
21. Cromer, D. T.; Waber, J. T. *International Tables for X-Ray Crystallography*, Kynoch Press, Birmingham, England, **1974**, *4*, Table 2.2 A.
22. Ibers, J. A.; Hamilton, W. C. *Acta Crystallogr.* **1964**, *17*, 781.
23. Cromer, D. T.; Waber, J. T. *International Tables for X-Ray Crystallography*, Kynoch Press, Birmingham, England, **1974**, *4*, Table 2.3.1.
24. *TEXSAN - TEXRAY Structural Analysis Package*, Molecular Structure Corporation, **1985**.
25. Spialter, L.; Pappalardo, J. A. *The Acyclic Aliphatic Tertiary Amines*, Macmillan, New York, **1965**, 25.

26. Braun, J. V.; Klar, R. *Chem. Ber.* **1940**, *73B*, 1417.
27. Law, P. H. W.; Martin, J. C. *J. Am. Chem. Soc.* **1977**, *99*, 5490.
28. Dela, E. W.; Kasum, B.; Kirkbride, K. P. *J. Am. Chem. Soc.* **1987**, *109*, 2746.
29. Brown, H. C.; Heim, P. *J. Org. Chem.* **1973**, *38*, 912.
30. Lane, C. F. *Chem. Rev.* **1976**, *76*, 795.
31. Moore, S.; Tarnowski, T.; Newcomb, M.; Cram, D. J. *J. Am. Chem. Soc.* **1977**, *99*, 6398.
32. Tashiro, M.; Yamato, T. *J. Org. Chem.* **1985**, *50*, 2939.
33. Gutowsky, H. S.; Holm, C. H.; Saika, A.; Williams, G. A. *J. Am. Chem. Soc.* **1957**, *79*, 4596.
34. (a) Corriu, R. J. P.; Mazhar, M.; Poirier, M.; Royo, G. *J. Organomet. Chem.* **1986**, *306*, C5. (b) Corriu, R. J. P.; Kpoton, A.; Poirier, M.; Royo, G. *J. Organomet. Chem.* **1984**, *277*, C25.
35. Berry, R. S. *J. Chem. Phys.* **1960**, *32*, 933.
36. Gillespie, P.; Hoffman, P.; Klusacek, H.; Marquarding, D.; Pfohl, S.; Ramirez, F.; Tsolis, E. A.; Ugi, I. *Angew. Chem. Int. Ed. Engl.* **1971**, *10*, 687.
37. Maskill, H. *The Physical Basis of Organic Chemistry*, Oxford University Press, New York, **1985**, 253.
38. Robertson, R. E. *Progr. Phys. Org. Chem.* **1967**, *4*, 213.
39. (a) Pellerite, M. J.; Brauman, J. I. *J. Am. Chem. Soc.* **1983**, *105*, 2672. (b) Pellerite, M. J.; Brauman, J. I. *J. Am. Chem. Soc.* **1980**, *102*, 5993. (c) Olmstead, W. N.; Brauman, J. I. *J. Am. Chem. Soc.* **1977**, *99*, 4219.
40. Chandrasekhar, J.; Jorgensen, W. L. *J. Am. Chem. Soc.* **1985**, *107*, 2974.
41. Pitzer, K. S.; Donath, W. E. *J. Am. Chem. Soc.* **1959**, *81*, 3213.
42. Dewar, M. J. S.; Friedheim, J.; Grady, G.; Healy, E. F.; Stewart, J. J. P. *Organometallics* **1986**, *5*, 375.
43. Dewar, M. J. S.; Zoebisch, E. G.; Grady, G.; Stewart, J. J. P. *J. Am. Chem. Soc.* **1985**, *107*, 3902.
44. Dewar, M. J. S.; Jie, C. *Organometallics* **1987**, *6*, 1486.
45. Stewart, J. J. P. *J. Comp. Chem.* **1989**, *10*, 209.
46. Dewar, M. J. S.; Jie, C. *Organometallics* **1989**, *8*, 1544.
47. Jean, J.; Volatron, F. *An Introduction to Molecular Orbitals*, Oxford Univ. Press, New York, **1993**, 90.

(*Received* 16 *August* 1996; *accepted* 27 *March* 1997)